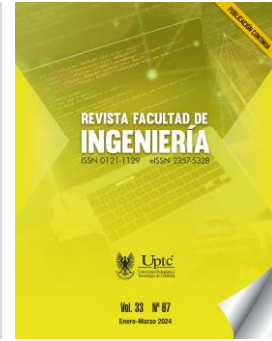


Revista Facultad de Ingeniería

Journal Homepage: <https://revistas.uptc.edu.co/index.php/ingenieria>



# Fourier Analysis Approach to Identify Water Bodies Through Hyperspectral Imagery

Gabriel-Elías Chanchí-Golondrino<sup>1</sup>

Manuel-Alejandro Ospina-Alarcón<sup>2</sup>

Manuel Saba<sup>3</sup>

**Received:** October 9, 2023

**Accepted:** February 19, 2024

**Published:** February 29, 2024

**Citation:** G.-E. Chanchí-Golondrino, M.-A. Ospina-Alarcón, M. Saba, "Fourier Analysis Approach to Identify Water Bodies Through Hyperspectral Imagery," *Revista Facultad de Ingeniería*, vol. 33, no. 67, e16328, 2024. <https://doi.org/10.19053/01211129.v33.n67.2024.17232>

## Abstract

Unlike conventional images, which have three channels of information, hyperspectral images are composed of many spectral channels that provide detailed information about the materials present in them. Thus, considering their great potential to monitor changes in the environment and the importance of freshwater

<sup>1</sup> Ph. D. Universidad de Cartagena  (Cartagena-Bolívar, Colombia). [gchanchig@unicartagena.edu.co](mailto:gchanchig@unicartagena.edu.co). ORCID: [0000-0002-0257-1988](https://orcid.org/0000-0002-0257-1988)

<sup>2</sup> Ph. D. Universidad de Cartagena  (Cartagena-Bolívar, Colombia). [mospinaa@unicartagena.edu.co](mailto:mospinaa@unicartagena.edu.co). ORCID: [0000-0003-4510-0753](https://orcid.org/0000-0003-4510-0753)

<sup>3</sup> Ph. D. Universidad de Cartagena  (Cartagena-Bolívar, Colombia). [msaba@unicartagena.edu.co](mailto:msaba@unicartagena.edu.co). ORCID: [0000-0003-1345-9657](https://orcid.org/0000-0003-1345-9657)



bodies for life and nature, it is relevant to propose and evaluate the effectiveness of different computational methods focused on detecting bodies of water in hyperspectral images; therefore, this research proposes and evaluates a computational method based on Fourier phase similarity. To do so, four methodological phases were defined, namely: exploration and selection of open-source technologies for hyperspectral image analysis, determination of the characteristic pixel of water bodies, calculation of Fourier phase similarity between the representative pixel of water bodies and the 200 sample pixels chosen from water bodies and other materials, and verification of the method on a test hyperspectral image. Spectral, NumPy, and Pandas libraries of Python were used to implement the proposed method, which resulted, for the first 170 bands, on an average phase similarity of 99.46% with respect to water body pixels and a minimum phase similarity with water body pixels of 93.01%. The results show that the proposed method is effective to detect water body pixels and can be used or extrapolated as an alternative to detection methods based on correlation metrics and machine learning.

**Keywords:** computer vision; Fourier analysis; hyperspectral imaging; machine learning; remote sensing; water bodies detection.

### **Enfoque de análisis de Fourier para la identificación de cuerpos de agua a través de imágenes hiperespectrales**

#### **Resumen**

A diferencia de las imágenes convencionales, las cuales cuentan con tres canales de información, las imágenes hiperespectrales están conformadas por una gran cantidad de canales espectrales que permiten brindar información detallada sobre diferentes materiales presentes en ellas. De este modo, teniendo en cuenta el gran potencial que tienen estas imágenes en la monitorización de cambios en el ambiente y considerando la importancia de los cuerpos de agua dulce para la vida y la naturaleza, es relevante proponer y evaluar la efectividad de diferentes métodos computacionales enfocados en la detección de cuerpos de agua en imágenes hiperespectrales. Por ende, el objetivo de esta investigación es proponer y evaluar

un método computacional basado en la similitud de fase de Fourier para la detección de cuerpos de agua en éstas. Para esto, fueron definidas cuatro fases metodológicas: exploración y selección de tecnologías libres para el análisis de imágenes hiperespectrales, determinación del pixel característico de los cuerpos de agua, cálculo de la similitud de fase de Fourier entre el pixel representativo de los cuerpos de agua y los 200 pixeles de muestra escogidos de cuerpos de agua y otros materiales, y verificación del método en una imagen hiperespectral de prueba. El método propuesto fue implementado mediante el uso de las librerías *Spectral*, *NumPy* y *Pandas* de *Python*, obteniendo como resultado para las primeras 170 bandas una similitud de fase promedio de 99,46% con respecto a pixeles de cuerpos de agua y una similitud de fase mínima con pixeles de cuerpos de agua de 93,01%. Los resultados permiten concluir que el método propuesto es efectivo para detectar pixeles de cuerpos de agua y puede ser usado o extrapolado como alternativa a los métodos de detección basados en métricas de correlación y *machine learning*.

**Palabras clave:** análisis de Fourier; aprendizaje automático; detección de cuerpos de agua; imágenes hiperespectrales; sensado remoto; visión por computador.

### **Abordagem de análise de Fourier para identificação de corpos d'água por meio de imagens hiperespectrais**

#### **Resumo**

Ao contrário das imagens convencionais, que possuem três canais de informação, as imagens hiperespectrais são compostas por um grande número de canais espectrais que permitem fornecer informações detalhadas sobre os diferentes materiais nelas presentes. Assim, tendo em conta o grande potencial que estas imagens têm na monitorização de alterações no ambiente e considerando a importância dos corpos de água doce para a vida e a natureza, é relevante propor e avaliar a eficácia de diferentes métodos computacionais focados na detecção de corpos de água em imagens hiperespectrais. Portanto, o objetivo desta pesquisa é propor e avaliar um método computacional baseado na similaridade de fases de Fourier para detecção de corpos d'água neles. Para isso foram definidas quatro fases metodológicas: exploração e seleção de tecnologias livres para análise de

imagens hiperespectrais, determinação do pixel característico dos corpos d'água, cálculo da similaridade de fase de Fourier entre o pixel representativo dos corpos d'água e o 200 pixels de amostra escolhidos em corpos d'água e outros materiais, e verificação do método em uma imagem hiperespectral de teste. O método proposto foi implementado através da utilização das bibliotecas Spectral, NumPy e Pandas Python, obtendo como resultado para as primeiras 170 bandas uma similaridade de fase média de 99,46% em relação aos pixels de corpos d'água e uma similaridade de fase mínima com pixels de corpos de água de 93,01%. Os resultados permitem concluir que o método proposto é eficaz para detecção de pixels de corpos d'água e pode ser utilizado ou extrapolado como alternativa aos métodos de detecção baseados em métricas de correlação e aprendizado de máquina.

**Palavras-chave:** análise de Fourier; aprendizado de máquina; detecção de corpos d'água; imagem hiperespectral; sensoriamento remoto; visão computacional.

## I. INTRODUCTION

Advanced technologies such as hyperspectral imaging play a pivotal role in detecting and categorizing materials within diverse landscapes [1]. Hyperspectral images, obtained through remote sensing techniques by aerial sensors and electromagnetic radiation, provide comprehensive spatial, temporal, and spectral information without physical contact [2]. These images encompass the solar reflectance region and span the visible spectrum (VIS), visible infrared (NIR), and shortwave infrared (SWIR) to generate data cubes that integrate spatial and spectral dimensions [3].

Hyperspectral images have demonstrated versatile applications across various domains, enhancing situational awareness in military surveillance by providing detailed information in security contexts [4]. For instance, the precise identification and monitoring of specific terrain features or potential threats have been proven valuable in military operations. Hyperspectral imaging facilitates early and accurate diagnosis in crop disease detection. Farmers and agricultural experts can swiftly implement targeted interventions by analyzing the unique spectral signatures associated with diseased crops [5-7]. The use of hyperspectral images has significantly enhanced forest management practices, particularly in the monitoring and control of forest resources; these images aid in assessing their health, identifying areas susceptible to diseases or pests, and planning effective conservation strategies [8, 9]. Environmental monitoring applications are diverse and impactful. Hyperspectral images play a crucial role in tracking changes in terrestrial temperature and enable the identification of temperature variations across landscapes [10, 11]. In the case of oceanic observations, these images assist in monitoring sea surface conditions and studying the impact of climate change on marine ecosystems [12]. Submarine topography assessment is another noteworthy application [13]. Hyperspectral images aid in mapping the underwater terrain by providing valuable information for oceanographers and geologists studying the geological features of the seabed. These examples underscore the versatility and efficacy of hyperspectral imaging across many applications, showcasing its successful implementation in various scientific and practical contexts [14].

Despite their widespread use, efficiently processing the substantial data volumes generated by hyperspectral images remains a significant challenge, especially when aiming at precise identification and characterization of water bodies based on spectral signatures. In this context, the need to propose innovative methods that enhance efficiency and reduce computational load becomes crucial. Supervised machine learning techniques, often used for material detection, demand ample training samples for model development [15, 16]. Thus, evaluating and comparing computational approaches becomes imperative to ensure accurate water body detection in hyperspectral images based on spectral signatures. In the field of hyperspectral image analysis, distance/correlation metrics and machine learning are extensively explored methodologies for material detection [17]. While these approaches are well-established, Fourier analysis-based methods have received comparatively less attention despite their potential to decompose spectral signals and unveil hidden patterns [18].

This article addresses the research gap by proposing a novel method based on Fourier analysis, specifically using Fourier phase similarity, to identify and detect water bodies in hyperspectral images. The efficacy of the method was assessed by comparing characteristic water pixels with non-water pixels across 380 frequency bands. It was validated on a hyperspectral image of a specific geographical area by open-source Python libraries such as Spectral, Pandas, NumPy, and Matplotlib. The findings of this study contribute to the academic and research landscape by providing a foundation to implement innovative water body detection methods in environmental contexts. The proposed approach aims to enhance the temporal monitoring of water distribution in urban settings.

Subsequent sections of this paper delve into the methodological phases, present the results, and conclude with insights for future work. They are structured as follows: the methodology section outlines the various methodological phases employed to conduct the current research. The results and discussion section provides an overview of the study findings, encompassing the identification of the characteristic water pixel, the method's assessment using a designated set of test pixels (comprising 100 water pixels and 100 non-water pixels), and the validation process

using a hyperspectral image representative of the Manga neighborhood in Cartagena de Indias. The last section offers the conclusions drawn from this research and prospects for future work.

## II. METHODOLOGY

To carry out the present research, we defined four methodological phases: exploring and selecting open-source technologies for hyperspectral image analysis, determining the characteristic or representative pixel of water bodies, calculating the Fourier phase similarity between the representative pixel of water bodies and the 200 selected pixels (100 water body pixels and 100 other material pixels), and verifying the method on a test hyperspectral image (Figure 1).

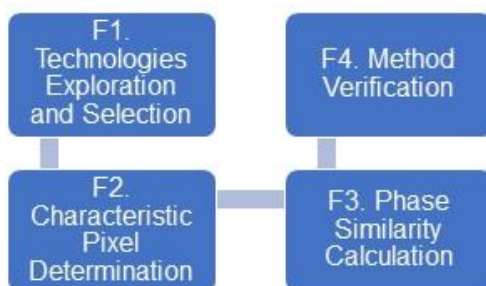


**Fig. 1.** Employed methodology.

According to Figure 1, in phase 1 of the methodology, a set of Python language libraries was selected to analyze and process hyperspectral images, including Spectral, NumPy, and Matplotlib. The Spectral library was used to read and process different bands or layers used in the study. The NumPy library was employed to determine the Fourier phase similarity between pixels. Finally, the Matplotlib library was used to generate graphs corresponding to the spectral signatures of bodies of water and other sample materials.

In Phase 2, from a hyperspectral image of the Manga neighborhood in Cartagena (1500 pixels wide and 1500 pixels high, each pixel with 380 reflectance bands), 100 pixels corresponding to bodies of water and 100 pixels to other materials (vegetation, concrete, containers, sea, among others) were sampled. Water body pixels served

to determine a characteristic or average pixel, which was then employed to calculate the phase similarity with the sample pixels.

Phase 3 involved calculating the Fourier phase similarity between the characteristic pixel identified in Phase 2 and the sample with both the 100 water body pixels and the 100 other material pixels. This process aimed to assess the accuracy of the proposed method and its capability to distinguish water pixels. The phase similarity calculation used various groups of bands due to the method's inability to fully distinguish water pixels using the entire set. Consequently, this phase established a threshold to detect water pixels.

It should be noted that the calculation of phase similarity involved obtaining the Fourier transform in advance by taking advantage of the NumPy library's functionalities for both the characteristic pixel and the other pixels to be processed. Equation (1) presents the mathematical representation of the Fourier transform applied to a specific pixel of the hyperspectral image. Fast Fourier Transform (FFT) is a highly effective algorithmic procedure, from a computational perspective, for the numerical evaluation of the Discrete Fourier Transform (DFT). Its inherent efficiency lies in the significant reduction of the calculation time required to obtain the DFT compared to traditional methods [19, 20].

$$X(k) = \frac{1}{N} \sum_{n=0}^{N-1} x(n) \cdot e^{-j \frac{2\pi}{N} k \cdot n} \quad (1)$$

Here,  $x(n)$  represents the spectral signature of the image as a function of the band  $n$ ,  $k$  is the spectrum phase, and  $N$  refers to the number of bands in each hyperspectral image. Likewise, the phase similarity calculated between the fast Fourier transforms of each pixel is presented mathematically in Equation (2) [21, 22].

$$\text{similarity}(Y_1, Y_2) = \frac{1}{N} \sum_f e^{j\Delta\phi_f} \times 100 \quad (2)$$

Where  $Y_1$  and  $Y_2$  are the Fourier transforms of the 2 correlated pixels,  $N$  represents the total number of frequencies in the signals  $Y_1$  and  $Y_2$ ,  $\sum_f$  is the sum of all frequencies, while  $\Delta\phi_f$  is the phase difference at frequency  $f$  defined according to Equation (3) [23]:

$$\Delta\phi_f = \angle Y_1(f) - \angle Y_2(f) \quad (3)$$

In Equation (3),  $e^{j\Delta\phi_f}$  is the complex exponential of the phase difference at frequency  $f$ . Thus, Equation (2) calculates the similarity between the phases of the two signals

at each frequency to determine the average of these values at all frequencies [24]. Finally, in phase 4 and to verify the effectiveness of the proposed method, iteration was performed for each pixel of the test hyperspectral image of the Manga neighborhood in Cartagena (Figure 2). The similarity with the reference pixel was determined to classify each pixel as belonging to water bodies or not. To do so, we used the detection threshold obtained in Phase 3. This image consists of a total of 2,250,000 pixels, with 380 reflectance bands each.



**Fig. 2.** Hyperspectral test image considered in the study.

### **III. RESULTS**

As previously mentioned in the methodology section, the study initially obtained a sample of 100 pixels corresponding to water bodies and 100 pixels of other materials from the hyperspectral test image presented in Figure 2, to evaluate the effectiveness of the method to distinguish water body pixels from other types of pixels. Thus, in Figure 3, the 100 sample pixels selected for water bodies are drawn on the test image in blue, while the 100 sample pixels selected for other types of materials (seawater, roofs, containers, roads, cars, among others) are shown in red.

## Fourier Analysis Approach to Identify Water Bodies Through Hyperspectral Imagery

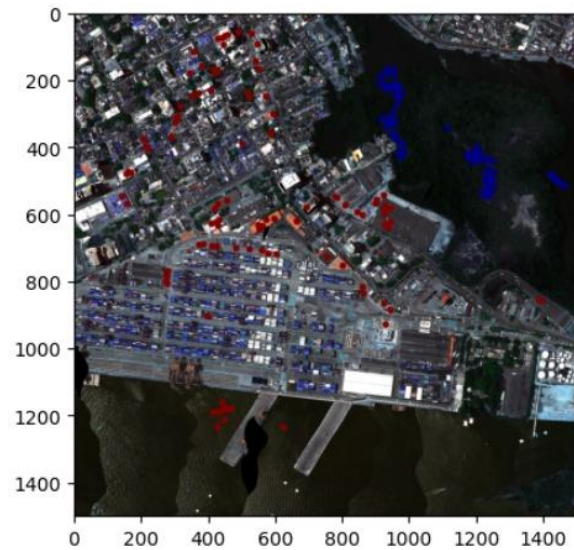


**Fig. 3.** Sample pixels considered.

From the 100 pixels corresponding to water bodies, the characteristic pixel or reference pixel was obtained, representing the spectral signature of the water bodies, by averaging the different bands of these pixels using the NumPy library. Thus, in Figure 4, it is possible to appreciate both the characteristic pixel and the 100 water body pixels that gave rise to it.

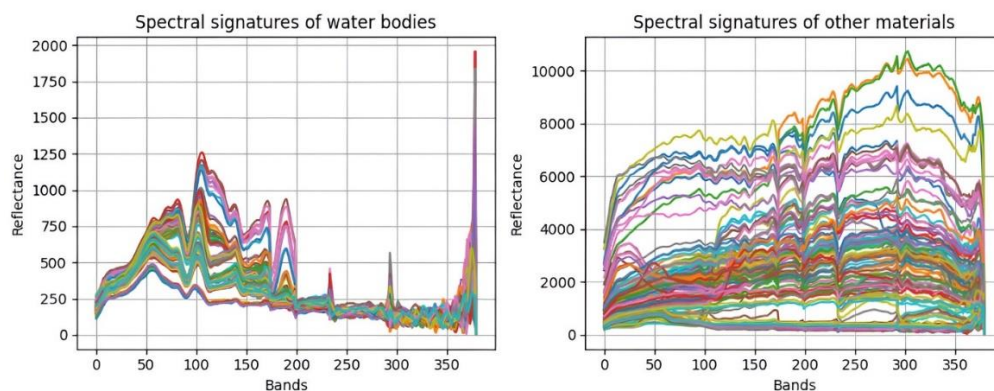


**Fig. 4.** Characteristic pixels of water bodies.

Based on the characteristic pixel presented in Figure 4, it is possible to calculate the phase similarity between the average pixel and the 100 sample pixels corresponding to water bodies and other materials by computational implementation of Equations (1)-(3). Thus, Figure 5 presents the implementation of the Fourier phase similarity in

the Python language. It is possible to observe that this function receives as parameters the Fast Fourier Transforms (FFT) of the two pixels between which the phase similarity will be calculated, in this case, the characteristic pixel and the sample pixels.

```
[24]: def sim_phase(Y1,Y2):
      p1 = np.angle(Y1)
      p2 = np.angle(Y2)
      #Determination of phase similarity
      phase_sim=np.mean(np.exp(1j*(p1-p2)))
      a=phase_sim.real
      b=phase_sim.imag
      sim=math.sqrt(a**2 + b**2)
      return sim*100
```

**Fig. 5.** Python implementation of Fourier phase similarity.

Furthermore, Figure 6 presents the FFT obtained for the characteristic pixel of water bodies: the x-axis shows the different frequency bands considered for each pixel; the y-axis shows the magnitude obtained for the frequency. The function shown in Figure 5 uses this transform as a parameter.

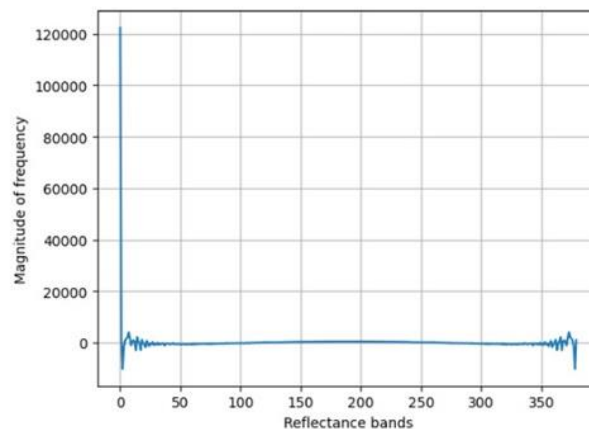


**Fig. 6.** Fast Fourier Transform of the characteristic pixel.

Considering that overlaps could occur in the similarity between the characteristic pixel and the sample pixels (water bodies and other materials), the experiment was replicated with 380 bands, with the first 300 bands, with the first 200 bands, and with the first 170 reflectance bands; the best results were obtained with 170 reflectance

bands. Figure 7 shows the average similarity, the maximum value, and the minimum value of similarity between the characteristic pixel and the pixels corresponding to water bodies for the aforementioned groups of bands.

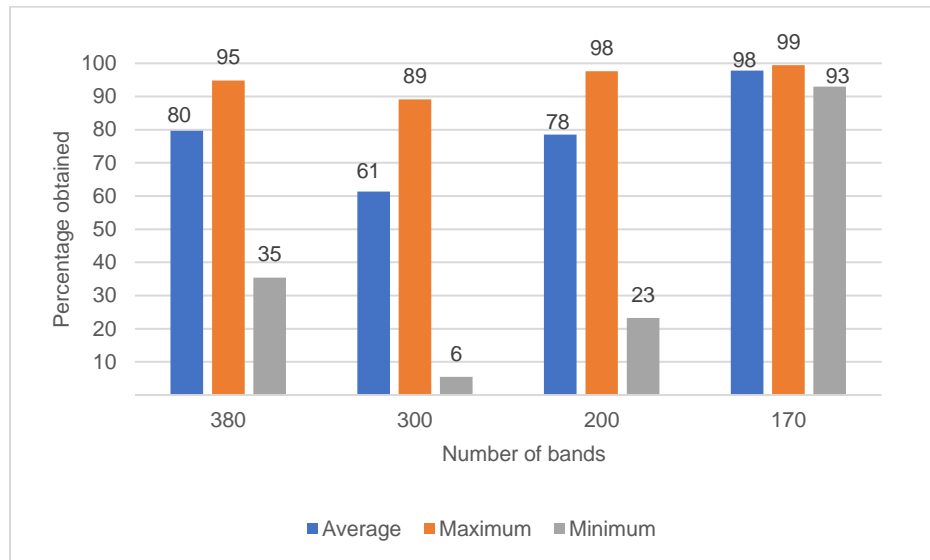
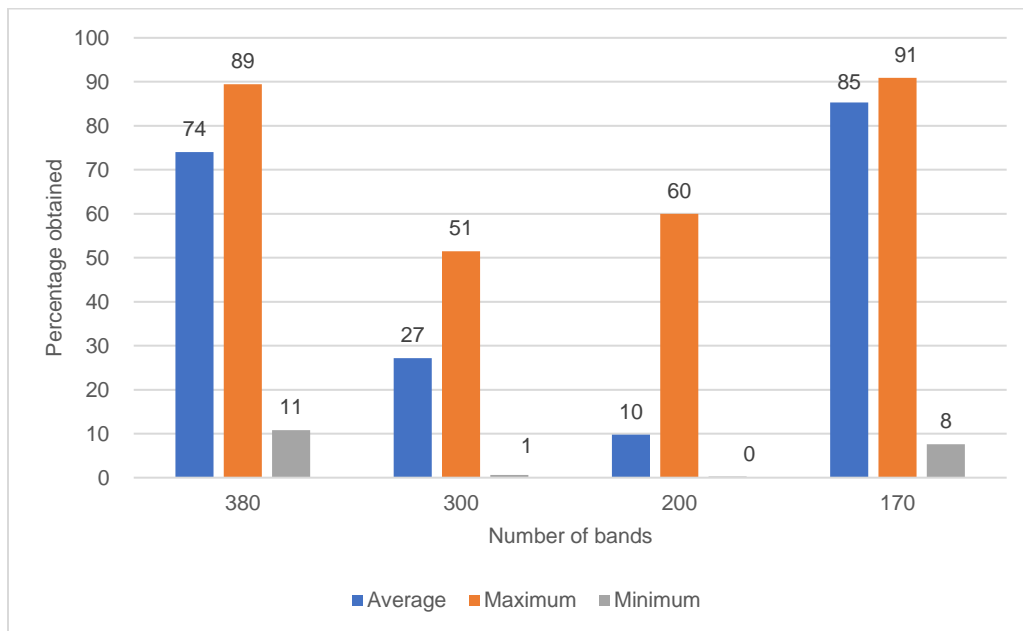


Fig. 7. Phase similarity for water bodies pixels at different bands.

Figure 7 also shows how the best results in the 3 statistical measures (minimum, maximum, and average) were obtained by the group with 170 bands. In all three cases, the similarity values are higher than 93%. In the case of the 200 bands, it is possible to appreciate a good result in the maximum value of similarity with 97.65%. However, the minimum value is 23.25%, so there is a high probability that this similarity overlaps with the similarities calculated for the other material pixels. Likewise, the minimum similarity values of the groups with 380, 300, and 200 bands oscillate between 5.50% and 35.37%, so that the Fourier phase similarity is not considered significant. The results evidence that the shape of the spectral signature presents peaks that differentiate them at the first 170 bands from the other material pixels, which can be seen more clearly in Figure 4.

Moreover, Figure 8 shows the phase similarities obtained between the characteristic pixel and the sample of 100 other material pixels at different reflectance bands. As a crucial criterion to determine the band count where the method exhibits the best efficacy, it is important to note that the maximum similarity value obtained with other

material pixels does not exceed the minimum value obtained with water body pixels. Thus, Figure 8 also shows that, despite the lower maximum similarity values between the characteristic pixel and other material pixels were obtained by the groups of the first 300 and 200 reflectance bands (51.49% and 59.97%, respectively), they have low minimum phase similarity values between the characteristic pixel and water body pixels (5.50% and 23.25, respectively). Hence, within these band groups, the method tends to misclassify water body pixels.



**Fig. 8.** Phase similarity for other material pixels at different bands.

A similar situation is seen in the case of the total bands, as the maximum phase similarity value between the characteristic pixel and other material pixels is 89.47%, whereas the minimum phase similarity value between the characteristic pixel and water body pixels is 35.37%, thus resulting in an overlap in the detection of water pixels. Finally, although in the case of the first 170 bands, the highest maximum similarity value is obtained between the characteristic pixel and other material pixels with a percentage value of 90.87%, it does not overlap with the minimum similarity obtained between the characteristic pixel and water body pixels, which is 93.01% (Percentage difference of 2.14% in similarity). Thus, for the first 170 bands, the proposed method was the most efficient in detecting water body pixels.

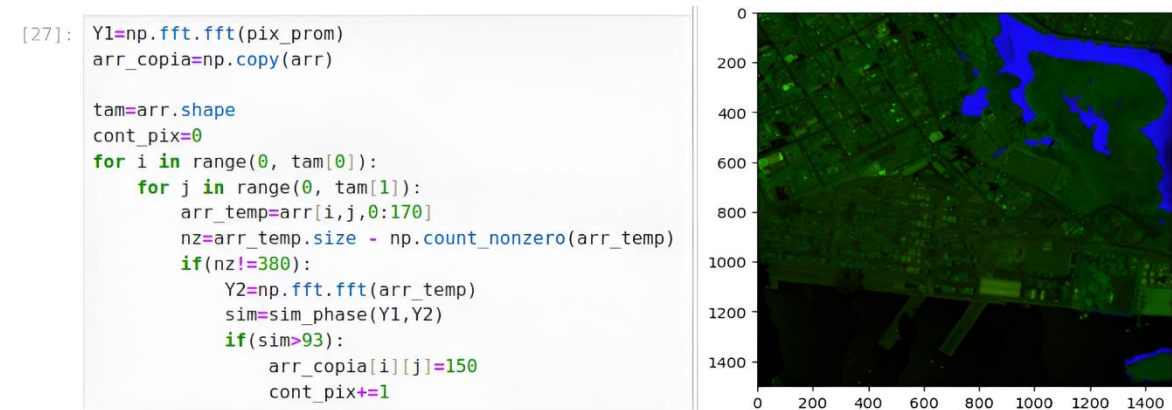


**Fig. 9.** Proposed method application on the test image.

The results obtained in the experiments described above determined a phase similarity detection threshold for water body pixels of 93.01%, considering the first 170 bands of the hyperspectral image, which also optimizes the computational performance of the method. Thus, by using the determined threshold, iteration was performed on each of the 2,250,000 pixels in the first 170 bands of the test hyperspectral image of the Manga neighborhood in Cartagena, determine whether it corresponds to a water body by phase similarity. Thus, Figure 9 illustrates the implemented algorithm and the resulting image; the areas where the algorithm detected water bodies are depicted in blue. It is possible to observe that the detected zones in the image visually correspond to the areas where freshwater bodies are located.

Similarly, upon counting the pixels comprising the detected water bodies, it was determined that the proposed method based on Fourier phase similarity identified 117,244 water pixels. This account for 5.21% of the total pixels in the analyzed image. Such a discovery underscores the need to rigorously evaluate material detection methods in hyperspectral images, especially in environmental contexts, as they enable monitoring and tracking the evolution of water bodies over time. This monitoring is essential for better understanding environmental changes and making informed decisions for management and conservation of these crucial water resources.

#### IV. DISCUSSION AND CONCLUSIONS

It is worth noting that compared to the results from [25], which evaluated vegetation detection methods using common approaches like distance and correlation metrics, our method, based on Fourier phase similarity calculation, achieved equal or higher similarity values. This suggests that our method presents a valid alternative for material detection in hyperspectral images. Nevertheless, the correlation metrics were effective with the total number of bands [25], while in this article, it was necessary to detect the most relevant number of bands to detect water bodies. This implies additional pre-processing work depending on the material with which the tests are being performed.

However, processing times decrease once the characteristic pixel is determined, and the optimum number of reflectance bands is obtained. Likewise, given the lower number of bands and the fact that the proposed method calculations focus on a reduced number of phases using the fast Fourier transform, it demonstrates better computational efficiency compared to other approaches such as methods based on machine learning or correlation metrics.

This study has introduced a novel approach for water body detection in hyperspectral images, grounded in Fourier analysis, specifically in the phase similarity between the representative water body pixels and other pixels in the respective hyperspectral image. The results suggest that this method can be valuable in academic research, particularly in environmental studies, for identifying and tracking the distribution of water bodies and vegetation in urban environments.

While various private tools are available for analyzing and processing hyperspectral images within the framework of geographic information systems, this study emphasizes the utility and vast potential of open-source tools and technologies. In this regard, the Python libraries Spectral and Pandas were employed to process and access hyperspectral images' pixels and bands. For the implementation of the Fourier analysis-based method, the advantages offered by the functions of the Python library NumPy were leveraged. Lastly, for visualizing image pixels and presenting hyperspectral images, the Matplotlib and spectral libraries were used. This study aimed at establishing a benchmark in harnessing these tools to implement

detection methods in hyperspectral images within academic and research environments. This orientation towards open-source tools not only promotes accessibility and transparency in research but also facilitates collaboration and knowledge exchange within the scientific community.

The method proposed in this article achieved the best results with the first 170 bands of the image, obtaining an average similarity of 99.46% with water body pixels (Figure 7) and an average similarity of 85.28% with other material pixels, as presented in Figure 8. Additionally, the minimum threshold detected with water pixels was 93.01%, while the maximum threshold obtained with other material pixels was 90.87%. The above results indicated that, although these thresholds are close (2.14% difference), there was no overlap; hence, the method can be used to identify the spectral signature corresponding to water pixels. Moreover, not using all bands in water body detection not only improved the effectiveness of the method but also its computational efficiency.

As a future work stemming from the present research, we aim to: a) compare the computational efficiency of the proposed method with methods based on correlation and distance metrics; b) analyze the effectiveness of the proposed method to detect other types of materials, such as asbestos or different types of water; c) hybridize the method with parallel computing approaches to establish a comparative analysis of computational efficiency with respect to other material detection approaches in hyperspectral images.

### **AUTHORS' CONTRIBUTION**

**Gabriel-Elías Chanchí-Golondrino:** conceptualization; data curation; investigation; methodology; writing-original draft.

**Manuel-Alejandro Ospina-Alarcón:** investigation; writing-edit and review.

**Manuel Saba:** investigation; writing-edit and review.

### **FUNDING**

This article is considered a product within the framework of the project 'Development of a Comprehensive Strategy to Reduce the Impact on Public Health and the

Environment Due to the Presence of Asbestos in the Territory of the Department of Bolívar,' funded by the General Royalties System of Colombia (SGR) identified with code BPIN 2020000100366. The University of Cartagena, Colombia, and the asbestos-free Colombia Foundation carry out this project.

## ACKNOWLEDGMENTS

The authors would like to express their gratitude to Federico Frassy for his support in the management and classification of hyperspectral data; to Aiken Hernando Ortega Heredia, María Angélica Narváez Cuadro, Carlos Andrés Castrillón Ortiz, Michelle Cecilia Montero Acosta, Margareth Peña Castro, Carlos David Arroyo Angulo, Leydy Karina Torres Gil, David Valdelamar Martínez, and the rest of the research team for their logistical support and sample collection in the field. Also, the authors would like to thank Juan Manuel González from BlackSquare company for helping acquire hyperspectral data.

## REFERENCES

- [1] Z. A. Lone, A. R. Pais, "Object detection in hyperspectral images," *Digital Signal Processing*, vol. 131, e103752, 2022. <https://doi.org/10.1016/j.dsp.2022.103752>
- [2] A. Zahra *et al.*, "Current advances in imaging spectroscopy and its state-of-the-art applications," *Expert Systems with Applications*, vol. 238, e122172, 2024. <https://doi.org/10.1016/j.eswa.2023.122172>
- [3] D. R. Green, J. J. Hagon, C. Gómez, B. J. Gregory, "Using Low-Cost UAVs for Environmental Monitoring, Mapping, and Modelling: Examples From the Coastal Zone," in *Coastal Management*, 2019, pp. 465-501. <https://doi.org/10.1016/B978-0-12-810473-6.00022-4>
- [4] FlySight S.r.l., "Understanding Hyperspectral Imaging – Benefits, Use Cases & Examples," 2023.
- [5] J. Deng *et al.*, "Pixel-level regression for UAV hyperspectral images: Deep learning-based quantitative inverse of wheat stripe rust disease index," *Computers and Electronics in Agriculture*, vol. 215, e108434, 2023. <https://doi.org/10.1016/j.compag.2023.108434>
- [6] A. Matese, J. M. Prince Czarniecki, S. Samiappan, R. Moorhead, "Are unmanned aerial vehicle-based hyperspectral imaging and machine learning advancing crop science?," *Trends in Plant Science*, vol. 29, no. 2, pp. 196-209, 2024. <https://doi.org/10.1016/j.tplants.2023.09.001>
- [7] N. Noshiri, M. A. Beck, C. P. Bidinosti, C. J. Henry, "A comprehensive review of 3D convolutional neural network-based classification techniques of diseased and defective crops using non-UAV-based hyperspectral images," *Smart Agricultural Technology*, vol. 5, e100316, 2023. <https://doi.org/10.1016/j.atech.2023.100316>
- [8] N. Li, L. Huo, X. Zhang, "Using only the red-edge bands is sufficient to detect tree stress: A case study on the early detection of PWD using hyperspectral drone images," *Computers and Electronics in Agriculture*,

## Fourier Analysis Approach to Identify Water Bodies Through Hyperspectral Imagery

- vol. 217, e108665, 2024. <https://doi.org/10.1016/j.compag.2024.108665>
- [9] X. Zhao *et al.*, "Evaluating the potential of airborne hyperspectral LiDAR for assessing forest insects and diseases with 3D Radiative Transfer Modeling," *Remote Sensing of Environment*, vol. 297, e113759, 2023. <https://doi.org/10.1016/j.rse.2023.113759>
- [10] F. Castillo, L. Arias, H. O. Garcés, "Estimation of temperature, local and global radiation of flames, using retrieved hyperspectral imaging," *Measurement*, vol. 208, e112459, 2023. <https://doi.org/10.1016/j.measurement.2023.112459>
- [11] W. Song, Y. Fu, S. Zhao, Y. Zhao, H. Wang, Z. Wang, "Post-fire assessment of heating temperatures experienced by concrete using short video imaging, hyperspectral imaging and laser-induced breakdown spectroscopy," *Construction and Building Materials*, vol. 392, e131834, 2023. <https://doi.org/10.1016/j.conbuildmat.2023.131834>
- [12] E. L. Hestir *et al.*, "Measuring freshwater aquatic ecosystems: The need for a hyperspectral global mapping satellite mission," *Remote Sensing of Environment*, vol. 167, pp. 181-195, 2015. <https://doi.org/10.1016/j.rse.2015.05.023>
- [13] T. Bajjouk *et al.*, "Detection of changes in shallow coral reefs status: Towards a spatial approach using hyperspectral and multispectral data," *Ecological Indicators*, vol. 96, pp. 174-191, 2019. <https://doi.org/10.1016/j.ecolind.2018.08.052>
- [14] L. K. Torres Gil, D. Valdelamar Martínez, M. Saba, "The Widespread Use of Remote Sensing in Asbestos, Vegetation, Oil and Gas, and Geology Applications," *Atmosphere (Basel)*, vol. 14, no. 1, e172, 2023. <https://doi.org/10.3390/atmos14010172>
- [15] R. Gong, J. Wang, X. Wang, Y. Liu, J. Shan, "Analysis of microplastics release from rice package in combination with machine learning and hyperspectral imaging technique," *Food Packaging Shelf Life*, vol. 39, e101152, 2023. <https://doi.org/10.1016/j.fpsl.2023.101152>
- [16] B. Graham Ram *et al.*, "Palmer amaranth identification using hyperspectral imaging and machine learning technologies in soybean field," *Computers and Electronics in Agriculture*, vol. 215, e108444, 2023. <https://doi.org/10.1016/j.compag.2023.108444>
- [17] J. Xu *et al.*, "Fuzzy graph convolutional network for hyperspectral image classification," *Engineering Applications of Artificial Intelligence*, vol. 127, e107280, 2024. <https://doi.org/10.1016/j.engappai.2023.107280>
- [18] H. Xie, J. Lu, J. Han, Y. Zhang, F. Xiong, Z. Zhao, "Fourier coded aperture transform hyperspectral imaging system," *Optics and Lasers in Engineering*, vol. 163, e107443, 2023. <https://doi.org/10.1016/j.optlaseng.2022.107443>
- [19] N. M. Francis, F. Pourahmadian, R. A. Lebensohn, R. Dingreville, "A fast Fourier transform-based solver for elastic micropolar composites," *Computer Methods in Applied Mechanics and Engineering*, vol. 418, e116510, 2024. <https://doi.org/10.1016/j.cma.2023.116510>
- [20] S. Wang, R. Tian, Q. Zhang, Z. Kang, X. Tang, "The application of trajectory analysis method and Fast Fourier Transform analysis method in the division of flow instability influence regions under ocean conditions," *Progress in Nuclear Energy*, vol. 168, e105045, 2024. <https://doi.org/10.1016/j.pnucene.2023.105045>
- [21] R. T. Leon, P. C. Sherrell, A. Šutka, A. V. Ellis, "Decoupling piezoelectric and triboelectric signals from PENGs using the fast fourier transform," *Nano Energy*, vol. 110, e108445, 2023. <https://doi.org/10.1016/j.nanoen.2023.108445>

- [22] O. Leitersdorf, Y. Boneh, G. Gazit, R. Ronen, S. Kvatinsky, "FourierPIM: High-throughput in-memory Fast Fourier Transform and polynomial multiplication," *Memories- Materials, Devices, Circuits and Systems*, vol. 4, e100034, 2023. <https://doi.org/10.1016/j.memori.2023.100034>
- [23] M. J. Spilsbury, A. Euceda, "Transformada Rápida de Fourier," *Revista de la Escuela de Física*, vol. 4, no. 2, pp. 45-52, 2019. <https://doi.org/10.5377/ref.v4i2.8276>
- [24] J. Semmlow, *Circuits, Signals and Systems for Bioengineers*. Elsevier, 2018. <https://doi.org/10.1016/C2015-0-06052-X>
- [25] G. E. Chanchí Golondrino, M. A. Ospina Alarcón, M. Saba, "Vegetation Identification in Hyperspectral Images Using Distance/Correlation Metrics," *Atmosphere (Basel)*, vol. 14, no. 7, e1148, 2023. <https://doi.org/10.3390/atmos14071148>